Linkage between Oligomerization and DNA Binding in *Drosophila* Doublesex Proteins†

Sayeon Cho‡ and Pieter C. Wensink*

The Rosenstiel Center and The Graduate Department of Biochemistry, Brandeis University, Waltham, Massachusetts 02254-9110

Received December 1, 1997; Revised Manuscript Received May 27, 1998

ABSTRACT: The doublesex gene of *Drosophila melanogaster* encodes DSX^M protein in males and DSX^F protein in females. Dimers of each protein bind a DNA site from which DSX^M represses and DSX^F activates transcription. Amino acids 1−397 are identical between the proteins and include a domain (DBD) for both DNA binding and protein oligomerization. The remaining nonhomologous and therefore sex-specific C-termini include an essential part of a second oligomerization domain. We have used mobility shift assays to investigate the effects these three oligomerization domains (DBD and two sex-specific) have on DSX dimerization and DNA binding. The intrinsic DNA binding affinities of DSX^M and DSX^F dimers are indistinguishable from each other (0.17 ± 0.04 nM) and slightly lower than that of DBD dimers (0.48 nM). In contrast, the dimerization dissociation constants of DSX^M (0.05 ± 0.02 nM) and DSX^F (0.16 ± 0.05 nM) are slightly different, but 4 orders of magnitude lower than that of DBD (430 nM). Thus sequences outside of DBD, presumably the sex-specific oligomerization domains, have substantial effects on apparent DNA binding affinity through thermodynamically linked effects on dimerization of full-length proteins. Further, when two DNA binding sites are adjacent, DBD dimers show no binding cooperativity, whereas full-length dimers bind with 2-fold different cooperativity (DSX^F, $k_{12} = 2.6$; DSX^M, $k_{12} = 5.4$). This suggests that the sex-specific domains may have a second effect on DNA binding, namely, an effect on binding cooperativity that depends on the number and arrangement of DNA sites.

The key interactions regulating transcription by polymerase II in higher organisms are between proteins and between proteins and DNA. In eukaryotes, protein factors that activate transcription typically have separate domains for activation and DNA binding. Once the DNA binding domain binds the factor to a DNA site, the activation domain(s) then interact directly or indirectly with proteins of the basal transcription complex (*1*−*3*). Currently, the mechanisms by which these domains activate are under intense investigation, so far revealing a plethora of activation targets within the basal transcription initiation complex of polymerase II and suggesting a variety of mechanisms (*3*−*5*). Repression of polymerase II transcription appears to be similarly complex and, in most cases, also to involve binding specific DNA sites near the promoter where the repressor either competes with activator proteins for DNA binding or has a more active role in which its repressor domain interacts directly or indirectly with activators, corepressors, or basal transcription factors (*6*).

The localization of a transcription factor to a promoter by the DNA binding domain often depends on dimerization of the factor because DNA binding domains of most factors are dimeric with more or less equal binding energy contributions from each half domain and strong binding cooperativity between the half domains. Different aspects of factor dimerization can have dramatic effects on DNA binding (*3, 6, 7*). For example, different homo- and heterodimers formed from a family of related monomers can have quite different DNA binding specificities (*8, 9*). On another level, relative dimer stabilities among different members of a family can determine whether a particular dimer is at sufficient concentration to bind a DNA site (*10*).

Protein interactions that stabilize binding to DNA are not limited to dimerization. If a transcription factor has insufficient DNA affinity to be biologically effective, protein interactions other than those allowing dimerization may come into play. For example, several identical dimers may bind cooperatively to repeated DNA sites near a promoter (*11*). Cooperative binding by nonidentical transcription factors has also been observed and is one basis for the combinatorial regulation that occurs during developmentally regulated transcription (*1, 10*).

In this study we examine the effects of three oligomerization domains on the oligomerization and DNA binding of two closely related transcription factors. The two transcription factors, male-specific DSX^M [1] and female-specific DSX^F proteins, regulate most of the sex-specific characteristics of the *Drosophila* body (reviewed in refs *12, 13*). These DSX proteins are encoded by alternatively spliced transcripts from the doublesex (dsx) gene (*14*). As shown in Figure 1, the first 397 amino acids are identical between the proteins and include a segment (amino acids 39−104) that contains both a DNA binding domain (DBD)

† This work was supported by National Institutes of Health Grant R01 GM46237.

* Author to whom correspondence should be addressed.

‡ Current address: Department of Pathology, Harvard Medical School, 200 Longwood Ave., Boston, MA 02115.

[1] Abbreviations: DSX^F and DSX^M, female and male doublesex proteins; DBD, DNA binding domain; OD1, oligomerization domain 1; $OD2^F$, $OD2^M$, and OD2, oligomerization domain 2 of females, males, and both; kb, kilobase(s); bp, base-pairs.

S0006-2960(97)02916-4 CCC: $15.00
Published on Web 07/17/1998

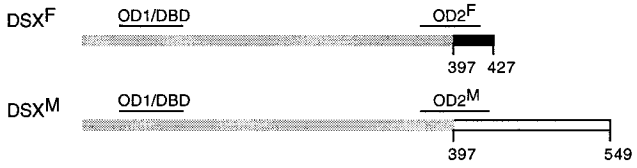

FIGURE 1: General structure of DSX proteins. Sequences common to male and female proteins (shaded boxes), only in females (filled box), and only in males (open box) are shown in this scale drawing. C-termini are indicated by vertical lines and amino acid numbers below the boxes. The locations of oligomerization and DNA binding domains are shown by horizontal lines.

and a protein oligomerization domain (OD1) (*15*−*17*). The sex-specific regulatory effects are all due to the very different C-termini (152 amino acids, DSX^M; 30 amino acids DSX^F). A second oligomerization domain, OD2, is near the carboxyl terminus and comes in two versions, one for each protein (OD2^F, 350−412; OD2^M, 350−427), with the sex-specific amino sequence of each being essential for OD2 oligomerization (*15*, *17*).

The best-characterized target for action of DSX protein is in a 33 bp enhancer that regulates the sex and tissue specificity of the yolk protein gene transcription in the fruit fly (*18*, *19*). Both proteins bind to the same site (dsxA) in this enhancer from which DSX^M represses transcription and DSX^F activates transcription in collaboration with proteins that bind to the two other sites of the enhancer.

Recent studies have shown that both DSX proteins form dimers at low protein concentration and have the ability to form tetramers and higher oligomers at high protein concentration (*20*). The dimers of DSX^M and DSX^F are the basic units for binding DNA. Studies of DSX protein dimer interactions with DNA have shown that both proteins are similar in their salt dependence, apparent affinities for the specific dsxA regulatory site, binding kinetics, and relative affinity for specific- and nonspecific-DNA sites (*21*).

To further examine the function of DSX proteins, we have now measured the dimerization constants, intrinsic DNA binding affinities, and DNA binding cooperativities of full-length proteins and DBD. The results indicate that DBD is responsible for all of the intrinsic DNA affinity of the full-length proteins. Sequences outside of DBD also contribute to DNA binding through thermodynamically linked effects on protein dimerization. The sex-nonspecific contribution of outside sequences is major, 4 orders of magnitude. The sex-specific effects are minor when the proteins bind to single DNA sites and cooperatively to adjacent DNA sites. We infer that OD2^F and OD2^M are responsible for most or all of these major and minor DNA binding effects.

MATERIALS AND METHODS

Proteins and DNAs. Full-length DSX proteins and DBD were overexpressed and purified from baculovirus-infected Sf9 cells (*15*, *21*). As assayed by Coomassie Blue staining of electrophoretic gels, the full-length proteins and DBD were approximately 90% and 50% pure, respectively. Throughout this paper the molarities of DSX^M, DSX^F, and DBD were calculated using the molecular weight of the dimer and the fraction of active protein as measured by mobility shift binding assays. All proteins were 60−70% active. Active protein concentrations were determined under stoichiometric conditions where concentrations of protein and DNA were at least 10-fold higher than the apparent equilibrium binding dissociation constants (Results; ref *21*). The dsxA sequence, the highest affinity binding site in the fat body enhancer of the yolk protein 1 gene (*19*, *22*), was synthesized, gel purified, ^{32}P end-labeled, and quantitated as described previously (*21*). To produce a fragment with two identical binding sites, the synthesized dsxA DNA was self-ligated and inserted into the *Sal*I site of pα1t[−157/+696] (*23*) from which the *Sal*I site upstream of −157 had been deleted. A 164 bp *Bam*HI/*Sal*I fragment containing two adjacent, oppositely oriented dsxA sites was excised from the plasmid and purified. The distance between centers of matches to the dsx consensus sequence (*19*) in these two dsxA sites is 40 bp. The resulting DNA fragment was ^{32}P-labeled and gel purified as described above.

Mobility Shift Assays. Gel electrophoresis mobility shift assays were as described previously with slight modifications (*21*). All binding reactions were 1 h, a time sufficient to reach equilibrium (*21*). Protein concentrations were kept below levels that saturate for DNA binding because protein aggregation occurs above approximately 25 nM for DBD and 0.5 nM for full-length protein, indicating that additional equilibria become quantitatively significant (*20*). The concentrations of total DNA in each binding reaction of an experiment were the same, and the sums of the radioactivity in bound and free DNA were within a few percent of being equal between all lanes of an experiment. For experiments examining K_1 and K_2, ^{32}P-labeled dsxA was at concentrations at least 40-fold lower (5 pM dsxA for full-length proteins and 0.12 nM for the DBD) than the apparent DNA binding dissociation constants (Results; ref *21*). For experiments examining binding cooperativity, the DNA fragment with two dsxA sites was at 1.0 pM. Therefore, in all experiments the concentration of total free protein is approximately equal to the concentration of protein added. Electrophoretic assays used nondenaturing polyacrylamide gels and were quantitated by the PhosphorImager (Molecular Dynamics).

In assays with DBD, poly(dI·dC)·poly(dI·dC) was added to reaction mixtures to prevent high-molecular-weight DBD aggregates. In the absence of this copolymer, such aggregates were detected in mobility shift assays even at low DBD concentrations. The molarity of poly(dI·dC)·poly(dI·dC) added was calculated in moles of nucleotides because each nucleotide in an average length (1 kb) copolymer represents a different binding site. Binding competition studies have shown that poly(dI·dC)·poly(dI·dC) binding sites have 10^6-fold lower affinity than dsxA for DSX protein (*21*) and for DBD (unpublished observations). The ratio of dsxA to copolymer was kept constant (10^5) in all DBD experiments to eliminate copolymer effects on binding.

Model for Protein−DNA Interaction and Protein Dimerization. To examine linkage between protein dimerization and dimer−DNA binding we made several assumptions. First, DNA binding affinity of monomers can be ignored because it is insignificant relative to dimers. Monomer−DNA complexes have not been detected by mobility shift assays over the DSX concentration range of 10^{-12} to 10^{-7} M. Second, monomers and dimers are in equilibrium. Third, no protein oligomers higher than dimers occur at the DSX concentrations used. No higher oligomeric forms bound to DNA were detected. Fourth, dissociation of protein−DNA complex is insignificant during gel electrophoresis. To

reduce dissociation, electrophoresis was sufficient only to separate complex from unbound DNA. Under this condition we found less than 5% of the DNA radiolabel between bands for the bound and unbound DNA. With these assumptions, the reaction can be described as

$$2P \underset{K_1}{\rightleftharpoons} P_2 \overset{D}{\underset{K_2}{\rightleftharpoons}} P_2D \quad (1)$$

where P, P_2, D, and P_2D are the monomer, dimer, DNA, and dimer−DNA complex, respectively. The dimerization dissociation constant, K_1, and the intrinsic DNA binding dissociation constant, K_2, are

$$K_1 = \frac{[P]^2}{[P_2]} \quad (2)$$

$$K_2 = \frac{[P_2][D]}{[P_2D]} \quad (3)$$

At any protein concentration, the experimental results expressed in terms of an apparent DNA binding dissociation constant, K_{app}, can be written as

$$K_{app} = \frac{[P]_f[D]}{[P_2D]} = \frac{[D]}{[P_2D]}\left(\frac{[P]}{2} + [P_2]\right) \quad (4)$$

where $[P]_f$ is total free protein concentration expressed in units of moles of dimer. By definition, K_{app} must vary with protein concentration because DNA binding is linked to protein dimerization (*24*).

Substituting eqs 2 and 3 into eq 4 yields

$$K_{app} = \frac{[D]}{[P_2D]}\left(\frac{1}{2}K_1^{1/2}\left(\frac{K_2[P_2D]}{[D]}\right)^{1/2} + \frac{K_2[P_2D]}{[D]}\right) \quad (5)$$

Rearranging yields

$$K_{app} = \frac{(K_1K_2)^{1/2}}{2}\left(\frac{[D]}{[P_2D]}\right)^{1/2} + K_2 \quad (6)$$

K_1 and K_2 were determined by plotting K_{app} against $([D]/[P_2D])^{1/2}$ as total protein concentration, $[P]_{Tot}$, was increased. K_{app} was determined with the assumption that $[P]_{Tot}$ was approximately equal to $[P]_f$ because the DNA concentrations in the equilibrium binding reactions were at least 40-fold lower than the apparent equilibrium dissociation constants.

The method for analyzing DBD data to estimate K_1 and K_2 used the same model. Its derivation began with a substitution for [P] in terms of $[P_2]$ and $[P]_{Tot}$ into eq 2

$$K_1[P_2] = [P]^2 = 4[P]_{Tot}^2 - 8[P]_{Tot}[P_2] + 4[P_2]^2 \quad (7)$$

$$4[P_2]^2 - (8[P]_{Tot} + K_1)[P_2] + 4[P]_{Tot}^2 = 0 \quad (8)$$

Applying the quadratic equation

$$[P_2] = \frac{8[P]_{Tot} + K_1 \pm \sqrt{K_1^2 + 16K_1[P]_{Tot}}}{8} \quad (9)$$

As $[P]_{Tot}$ approaches zero, $[P_2]$ goes to zero, therefore the positive square-root term is inappropriate. Rearranging eq 3 and substituting from eq 9

$$\frac{[P_2D]}{[D]} = \frac{8[P]_{Tot} + K_1 - \sqrt{K_1^2 + 16K_1[P]_{Tot}}}{8K_2} \quad (10)$$

Simplifying yields

$$\frac{[P_2D]}{[D]} = \frac{[P]_{Tot}}{K_2} + \frac{K_1}{8K_2}\left(1 - \sqrt{1 + \frac{16[P]_{Tot}}{K_1}}\right) \quad (11)$$

Binding Cooperativity. ^{32}P-labeled DNA containing two dsxA sites was incubated with various concentrations of protein. The resulting unbound, singly bound, and doubly bound complexes were then separated in mobility shift assays and quantitated by the PhosphorImager.

The analytical method is summarized here. It was essentially the method of Senear and Brenowitz (*25*) based on previous theoretical work (*24*, *26*). When protein dimers bind to sites 1 and 2 with the intrinsic binding association constants, k_1 and k_2, respectively, and the cooperativity parameter, k_{12}, for binding to two sites, the fraction of each complex, F_i, that is unbound (F_0), singly bound (F_1), and doubly bound (F_2) can be described as follows (Figure 5):

$$F_0 = \frac{1}{1 + (k_1 + k_2)[P_2] + k_1k_2k_{12}[P_2]^2} \quad (12)$$

$$F_1 = \frac{(k_1 + k_2)[P_2]}{1 + (k_1 + k_2)[P_2] + k_1k_2k_{12}[P_2]^2} \quad (13)$$

$$F_2 = \frac{k_1k_2k_{12}[P_2]^2}{1 + (k_1 + k_2)[P_2] + k_1k_2k_{12}[P_2]^2} \quad (14)$$

where $[P_2]$ is the concentration of free DSX protein dimer. $[P_2]$ of full-length proteins was calculated from dimerization constants and $[P]_f$. When DBD was used, $[P_2]$ was replaced with $4[P]_f{}^2/K_1$ where $[P]_f$ is the added protein concentration in dimer mass units and K_1 is the dimerization constant of the DNA binding domain, 430 nM (Figure 3), because in the concentration range used, monomer is in excess over dimer and the concentration of dimer bound to DNA is negligible.

The case examined in these experiments was simplified by the assumption that $k_1 = k_2$. This assumption appears justified since the two binding sites are identical and have identical sequence contexts (*25*). Association constants were obtained by fitting binding curves to data using the Delta-Graph 4.0 program (Delta-Point). An alternative estimate of the cooperativity parameter was made by measuring F_{1max}, the maximum value of F_1.

$$F_{1max} = \frac{k_1 + k_2}{2(k_1k_2k_{12})^{1/2} + k_1 + k_2} \quad (15)$$

If k_1 is equal to k_2, k_{12} can be written

$$k_{12} = \left(\frac{1}{F_{1max}} - 1\right)^2 \quad (16)$$

Therefore, if $F_{1max} = 0.5$, then $k_{12} = 1$, indicating no binding

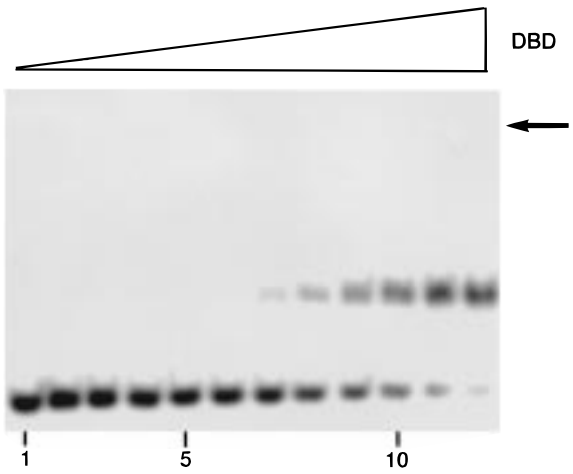

FIGURE 2: Binding between DBD and dsxA DNA. Autoradiogram of electrophoretic mobility shifts. ^{32}P-labeled dsxA DNA (0.12 nM) was titrated with increasing concentrations of DBD protein (0.74, 0.98, 1.31, 1.74, 2.32, 3.09, 4.13, 5.5, 7.3, 9.75, 13, and 26 nM, respectively, for lanes 1−12). The arrow indicates the location of the gel wells. The lower and upper bands are unbound and bound DNA, respectively.

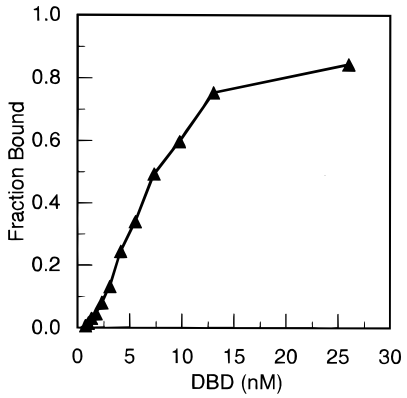

FIGURE 3: Apparent DNA binding affinity of the DBD. Electrophoretic mobility shift experiment of Figure 2 quantitated by the PhosphorImager. The concentration of protein at half-saturation is 7 nM, an estimator for the apparent dissociation constant. Titration was not carried beyond 85% of saturation because DBD aggregation occurs above 25 nM (Materials and Methods).

cooperativity. Lower values of F_{1max} indicate positive cooperativity, and higher values indicate negative cooperativity.

RESULTS

Apparent Affinity of DSX DNA Binding Domain for a Specific DNA Site. We measured the apparent binding equilibrium between DBD and dsxA DNA. The DBD was expressed in baculovirus-infected Sf9 insect cells, partially purified, and then incubated with radiolabeled dsxA, a regulatory site from the yolk protein genes. Previous work showed that DBD and full-length DSX proteins bind this dsxA site with the same high sequence specificity, but did not measure the equilibrium between DBD and dsxA (*15, 21*). Figures 2 and 3 show this binding as assayed by gel electrophoresis mobility shifts. The half saturation point is 7 nM, indicating that the apparent dissociation constant is approximately 40-fold higher than those of the full-length DSX proteins (*21*).

The sigmoidal shape of the DBD binding curve suggests a simple hypothesis for the difference between the apparent DNA dissociation constants of DBD and full-length protein: DSX sequences outside DBD contribute to dimerization energy and dimerization is thermodynamically linked to DNA binding. Supporting this hypothesis is the observation that for both DBD and full-length protein, dimers bind DNA but monomers have no detectable binding (*15, 21*). Further, two oligomerization domains have been detected in each of the full-length DSX proteins (Figure 1, refs *15, 17*). One of them, OD1, is in the N-terminal DBD. The other, OD2, is in a C-terminal region and includes sex-specific sequences that are essential for OD2 oligomerization. If this linkage hypothesis is correct, then DBD and full-length protein may have the same intrinsic DNA binding affinity, that is, the same affinity if each were exclusively in dimer form. If the linkage hypothesis is incorrect, then Figure 3 can only be explained by a DSX sequence outside DBD acting to increase the intrinsic DNA binding.

Thermodynamic Linkage between DSX Dimerization and DNA Binding. We investigated whether the change in apparent DNA binding affinity of DBD relative to DSX protein is due to a change in intrinsic DNA binding affinity or dimerization energy. We reasoned that since dimers and monomers are in equilibrium and dimers but not monomers have detectable binding to DNA, then the dimerization constant (K_1) and intrinsic DNA binding constant (K_2) can be determined from the ratio of bound to unbound DNA as total protein concentration is varied (Materials and Methods). In these experiments, electrophoretic mobility shift assays were used because they can detect DNA binding at the low concentrations of protein and DNA where the equations apply to DSX protein, that is, where higher order DSX oligomers are not a factor (*15, 20*).

Results from experiments with purified full-length proteins are shown in Figure 4A, a linear plot that gives direct visualization of the constants (Materials and Methods). To our knowledge this simple plotting method has not been used before. As expected, computer fitting of a curve to the data in a more standard sigmoidal plot gives the same results (Figure 4B; Materials and Methods). In four experiments with each full-length protein, the intrinsic DNA binding affinities (ordinate intercepts in Figure 4A) were statistically indistinguishable, $K_2 = 0.17$ (± 0.04) nM ($n = 8$). By contrast, dimerization constants derived from the slopes were slightly, but clearly different for the two proteins (Figure 4A). The K_1 for DSX^M, 0.05 (± 0.02) nM ($n = 4$), is approximately 3-fold lower than that for DSX^F, 0.16 (± 0.05) nM ($n = 4$). There is a 90% statistical confidence that these two K_1's are different. At protein concentrations higher than those used in these experiments, data become nonlinear, most likely because higher oligomers become significant and eq 1 no longer applies (*20*). These data show that DSX^M and DSX^F have the same intrinsic DNA binding affinities. The data also show that although the C-terminal, sex-specific sequences have no detectable effect on intrinsic binding, they have slightly different effects on dimerization.

To examine linkage between DNA binding and the dimerization energy provided by sequences outside of DBD, we also investigated dimerization and DNA binding of DBD. Figure 4C shows the data from two separate experiments fit by eq 11 (Materials and Methods). The dimerization

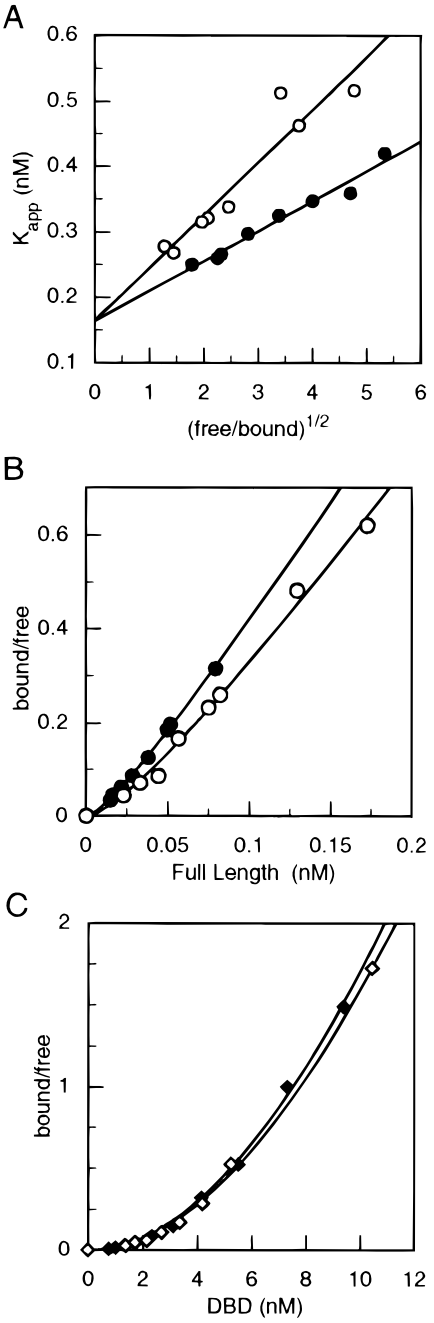

FIGURE 4: Dimerization and intrinsic DNA binding constants for DSX proteins. Panel A: Linear plot of mobility shift experiments assaying interactions between dsxA DNA (5 pM) and full-length DSX proteins (DSX^M, filled circles; and DSX^F, open circles; 1−200 pM). Panel B: Sigmoidal plot of data in panel A. Symbols are the same. The K_1 from the curve fits are 0.041 and 0.098 nM for DSX^M and DSX^F, respectively; the K_2, 0.17 and 0.18 nM for DSX^M and DSX^F, respectively. Panel C: Sigmoidal plot of interaction between DBD (filled and open diamonds are data from two independent experiments) and dsxA (0.12 nM). The R^2 regression coefficients are 0.971 and 0.999 (DSX^M), 0.901 and 0.994 (DSX^F) for panels A and B, respectively, and 0.998 (DBD, fit of data from both experiments) for panel C.

dissociation constant of DBD from these fits is 430 nM (422 and 440 nM), a value approximately 4 orders of magnitude higher than for full-length proteins. The intrinsic DNA binding dissociation constant for DBD is 0.48 nM (0.45 and 0.50 nM), 3-fold higher than for the full-length proteins.

Comparing results from DBD and DSX proteins shows that dimerization energy from amino acids outside of DBD

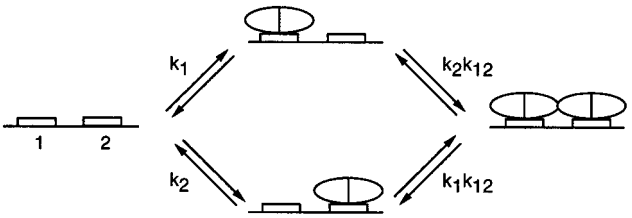

FIGURE 5: Model for binding DSX dimers to two adjacent dsxA sites. The intrinsic association constants, k_1 and k_2, represent the binding constants to DNA sites 1 and 2, while k_{12} is the cooperativity parameter representing the increased stability of protein−DNA complexes resulting from binding two protein dimers (represented by bisected ovals) to the two dsxA sites.

is thermodynamically linked to DNA binding. First, intrinsic DNA binding affinities of DBD and full-length proteins are less than 3-fold different. We conclude that interactions with dsxA DNA are likely to be limited to a protein structure that is identical in DSX^M, DSX^F, and DBD. Second, a comparison of dimerization energies shows that sequences outside DBD make a 10^4-fold contribution to dimerization and can substantially affect the K_{app} for DNA binding by full-length proteins. We presume these other sequences are in OD2 because OD2 is the only other oligomerization domain detected outside DBD

Cooperative Binding to Adjacent DNA Sites. There are several indications that DSX proteins cooperatively activate transcription in vivo from multiple sites separated by 1−4 helical turns of the DNA (*19, 22, 27*). In the best example, DSX^F activates from tandem copies of an enhancer element containing only dsxA and a binding site for another activator protein (*18*). In nonquantitative assays of β-galactosidase activity from a reporter gene, one of these enhancer elements has no activity, two spaced 43 bp apart have some activity, and four have strong activity. This transcriptional activation can be explained by cooperative binding by DSX or the other activator protein, or by cooperative interactions with the transcription initiation complex, or some combination of these. Supporting the possibility of cooperative binding by DSX, in vitro experiments show that at high protein concentration both DSX^M and DSX^F form tetramers in solution (*20*).

To investigate the possibility of cooperative DSX binding, we examined binding of each protein to two dsxA sites separated by 40 bp. A model for the binding interactions is diagrammed in Figure 5. Since mobility shift assays can detect all three species of DNA (unbound, singly bound, and doubly bound), we used the curve fitting method of Senear and Brenowitz to obtain all of the microscopic association constants (Materials and Methods). This treatment was simplified by assuming that k_1 and k_2 are the same, an assumption based on the identity of the two sites. The DSX protein concentrations used in the mobility shift assays were sufficiently low to prevent free protein from oligomerizing above the dimer level (*20*).

Figure 6 shows representative mobility shift assays for each of the three proteins. Curve fitting for DSX^M is shown in Figure 7A. The parameters determined by the curve fit confirm the intrinsic binding affinity determined in the previous section and also show that there is evidence for a small binding cooperativity. The intrinsic DNA binding dissociation constant ($K_2 = 1/k_1$) obtained by fitting data of

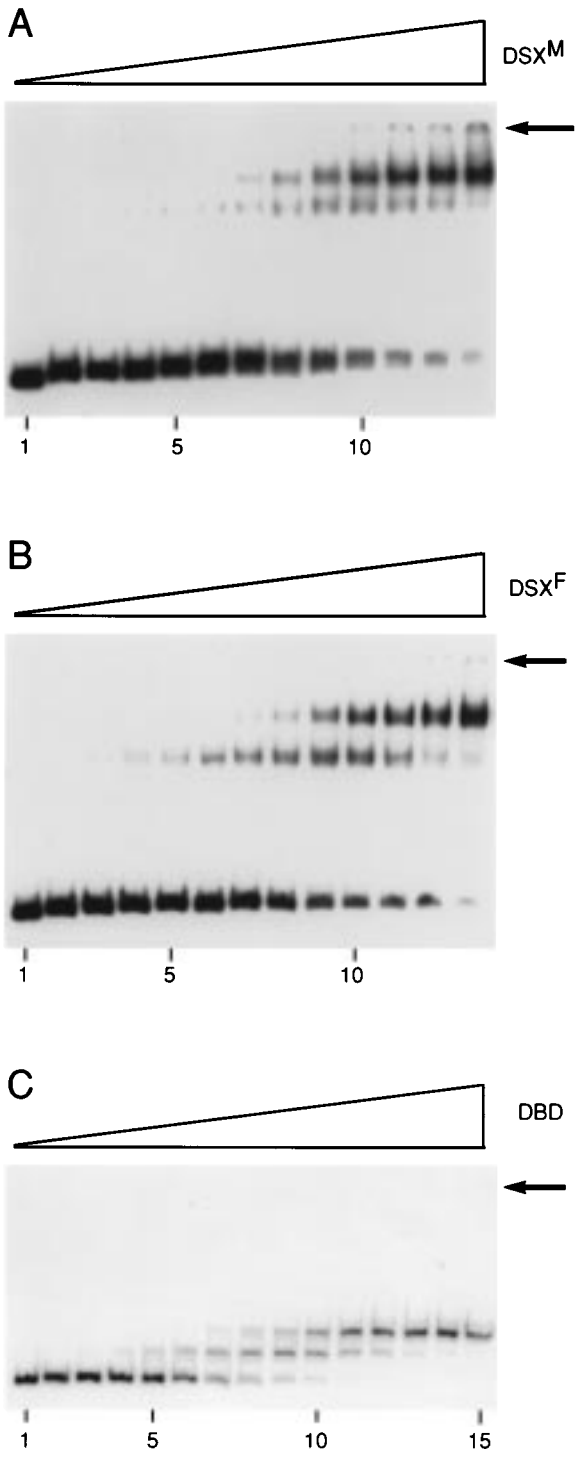

FIGURE 6: Binding of DSX proteins to adjacent dsxA sites. Autoradiograms of electrophoretic mobility shift assays of binding to a pair of dsxA sites by (A) DSX^M, (B) DSX^F, and (C) DBD proteins. The arrows indicate the location of gel wells. The bottom, middle, and top bands are unbound, singly bound, and doubly bound dsxA DNA.

the singly bound dsxA is 0.11 nM, similar to the value obtained in Figure 4A. In addition, the maximum fraction of singly bound molecule is 0.3, indicating cooperative binding (Figure 7A; Materials and Methods). The cooperativity parameter (k_{12}) calculated from this fraction is 5.4 (eq 16) and from the curve fitting, 4.9. Similar values for cooperativity parameters have been reported for other DNA-binding proteins (*11, 28, 29*).

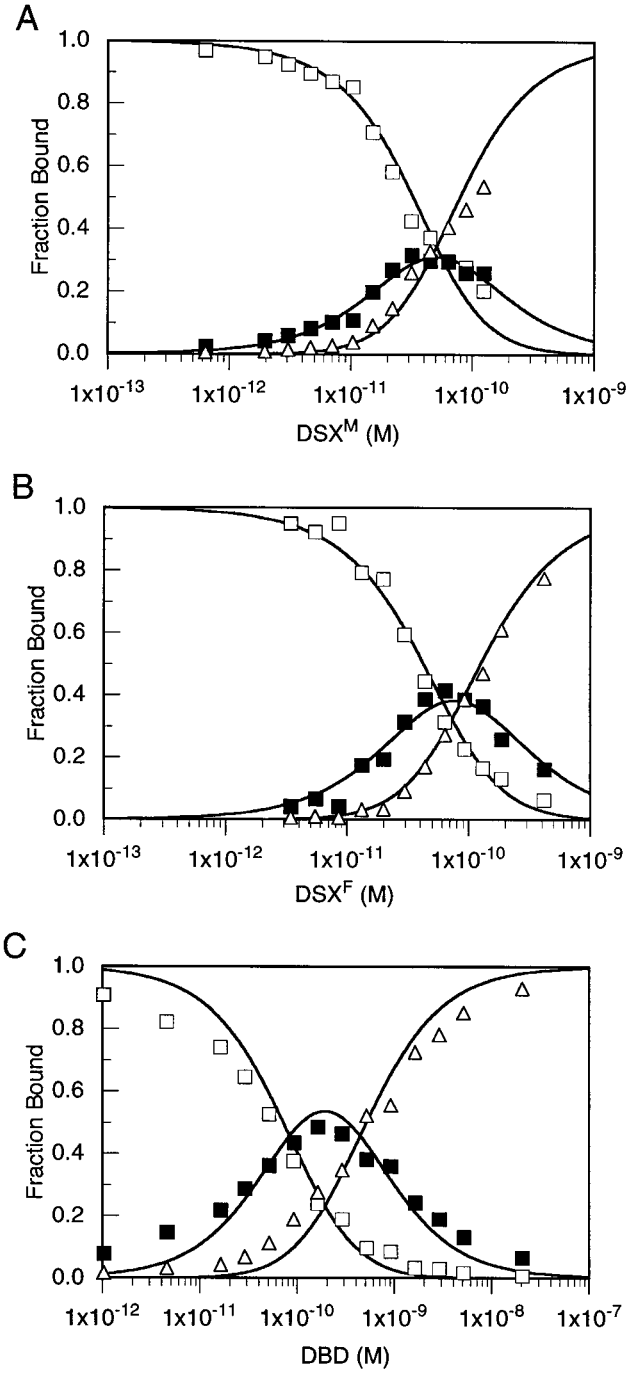

FIGURE 7: Determining binding cooperativity by curve fitting. Electrophoretic mobility shift assays of binding to a pair of dsxA DNA sites by (A) DSX^M, (B) DSX^F, and (C) DBD proteins. The ^{32}P-labeled DNA was incubated with protein for 1 h. Unbound (unfilled squares), singly bound (filled squares), and doubly bound (triangles) DNA are shown. Higher concentration of DBD and full-length proteins were not used because mobility shifts from protein aggregates were detected (Materials and Methods). The curves are drawn using eqs 12−14 using the k_1 and k_{12} from best fits of eq 13 to data points for singly bound DNA. The dimer concentrations shown on the abscissa are calculated from dimerization constants as described in Materials and Methods.

The same experimental approach showed that intrinsic binding by DSX^F was similar to DSX^M and cooperativity was 2-fold lower (Figure 7B). The intrinsic DNA binding dissociation constant of DSX^F calculated from the curve for singly bound dsxA is 0.12 nM, strengthening the conclusion reached in the previous section, namely, that DSX^M and

Table 1: Dimerization and DNA Binding Constants for DSX Proteins

	DBD	DSX^F	DSX^M
apparent DNA affinity ($K_{2,app}$; M)	7×10^{-9}	0.2×10^{-9} [a]	0.2×10^{-9} [a]
intrinsic DNA affinity (K_2; M)[b]	0.48×10^{-9}	0.17×10^{-9}	0.17×10^{-9}
intrinsic DNA affinity (K_2; M)[c]	0.17×10^{-9}	0.12×10^{-9}	0.11×10^{-9}
dimerization constant (K_1; M)[b]	430×10^{-9}	0.16×10^{-9}	0.05×10^{-9}
DNA binding cooperativity (k_{12})[d]	0.9	2.6	5.4

[a] From ref *21*. [b] From Figure 4. [c] From $1/k_1$, Figure 7. [d] From eq 16, Figure 7.

DSX^F have indistinguishable intrinsic DNA binding affinities. Cooperativity parameter estimates for DSX^F are 2.6 (eq 16) and 2.2 (curve fit), indicating that DSX^F binds with approximately 2-fold lower cooperativity than DSX^M (Figure 7B). This cooperativity result suggests that the sex-specific domains of both proteins are involved in protein dimerization and DNA binding cooperativity.

Next, we tested whether there is cooperativity in DBD binding (Figure 7C). The theoretical curves fit the data fairly well, although not as well as for the full-length protein. We suspect that there is a slight nonideality in dimerization at relatively high protein concentration. For examples, monomer binding to DNA or DNA mediated dimerization may become factors. Ignoring this, we used the curve parameters to estimate the intrinsic DNA binding constant, 0.17 nM, a value 3-fold lower than determined in Figure 4C and indistinguishable from the values for full-length proteins. The cooperativity parameter is 0.9 (eq 16) and 0.8 (curve fitting) indicating no cooperativity or small negative cooperativity.

In summary, these experiments provide evidence for binding cooperativity by full-length proteins, but none for DBD. While the detected cooperativity is small, it correlates with the small transcriptional activation cooperativity observed in vivo for two dsxA sites with similar spacing. It seems likely that additional binding sites, as occur in the natural dsxA enhancers, and optimized spacing of the sites would increase cooperativity. Whether this speculation is correct, the experiments described here indicate that the DBD is not responsible for this cooperativity, leaving the inference that OD2 is responsible.

DISCUSSION

Thermodynamic Linkage between DSX Dimerization and DNA Binding. We have used mobility shift assays to determine the intrinsic DNA binding affinities and protein dimerization constants for DSX proteins. As shown in Table 1, the intrinsic DNA binding affinities of DSX^M, DSX^F, and DBD are indistinguishable. This indicates that the intrinsic DNA binding affinity of the full-length proteins is determined by the DNA binding domain.

The dimerization and apparent DNA binding affinities of DSX proteins are more complex, as might be expected from two separate oligomerization domains, one sex-nonspecific and one sex-specific, being involved in dimerization of each full length protein. The dimerization constants of DSX^M and DSX^F are different and reproducible. However, the difference is small and needs to be confirmed by other methods. Our data show that DSX^M dimerizes 3-fold more strongly than DSX^F (Table 1). The OD1 oligomerization domain is included in the sex-nonspecific DBD, whereas the OD2 oligomerization domain is located at the boundary between sex-specific and sex-nonspecific regions and includes sex-specific amino acids that are necessary for oligomerization (*15*). Therefore, we infer that the small difference between the dimerization of the two full-length proteins comes from the sex-specific sequences in OD2.

Dimerization constant measurements for DBD indicate that it dimerizes poorly compared to full-length proteins. This suggests a simple explanation for the differences between the apparent DNA binding affinities of DBD and the full-length proteins (Table 1). Since the intrinsic DNA binding affinities of DBD and the full-length proteins are indistinguishable, the reduced apparent binding of DBD is most likely due to its reduced dimerization. It seems that the basic role of OD1 dimerization is to keep the two half sites for DNA binding together to form a unit that determines the intrinsic DNA binding affinity and specificity. A role for OD2 revealed in these studies is to provide the additional dimerization energy that allows dimerization of full-length monomers in the physiologically relevant nanomolar concentration range. This role has been preserved between $OD2^F$ and $OD2^M$ despite the highly nonconserved sequence in the carboxyl halves of these domains, both of which are essential for OD2 oligomerization.

Since OD1 and OD2 oligomerize independently, this appears to be a clear example of thermodynamic linkage between dimerization and protein−DNA binding. A thermodynamic linkage between dimerization and DNA binding has previously been demonstrated for *gal* repressor and for a *lac* repressor mutant (*30*−*32*). When the C-terminal coiled-coil interaction domain of the *lac* repressor is disrupted by a mutation that prevents formation of the normal tetramer, the dimers have an apparent DNA binding affinity that is reduced relative to wild-type tetramers. The reduction is due to decreased dimerization constant. The intrinsic DNA binding constants for the mutant dimer and wild-type tetramer are very similar, whereas with the mutant the equilibrium between the DNA binding species, the dimer, and the monomer is shifted toward the monomer (*32*).

Cooperativity of DSX Binding to Multiple DNA Sites. The binding results reported here not only support the possibility that both DSX^M and DSX^F bind to two adjacent sites cooperatively, but also indicate that DSX^M has 2-fold higher cooperativity than DSX^F (Table 1). This difference, together with the observations that DBD shows no binding cooperativity and that OD2 is the only other region that shows affinity between DSX proteins, suggests that OD2 may be responsible for the cooperativity of full-length proteins. Therefore, in addition to increasing the dimerization equilibrium to a physiologically relevant range as discussed in the previous section, a second role for OD2 may be to supply energy for cooperative binding to adjacent DNA sites.

DSX-Mediated Transcription Regulation in Vivo. The dsx binding sites (A, B1, B2, and C) in the 126 bp fat body

enhancer of *Yp* genes partially overlap bZIP protein binding sites (1, 2, and 3) (*19*). Among them, the dsxA site partially overlaps the bzip1 site to which a sex-nonspecific transcription activator binds. When these two sites are tetramerized, they activate transcription synergistically and specifically in female fat bodies and repress transcription in males (*18*). Although we detected only a 2.5- and 5-fold binding cooperativity when DSX^F and DSX^M bind to a pair of dsxA sites, cooperativity may be amplified in vivo by additional binding sites in the enhancer and by optimized spacing between sites. The function of cooperative binding in regulation remains a matter of speculation. One simple possibility is that the bZIP protein directly activates the transcription initiation complex, whereas DSX proteins determine the probability that bZIP binds to the enhancer. If this is the case, activation may occur because of a combination of DSX^F self-cooperative binding due to $OD2^F$ self-affinity and DSX^F/bZIP cooperative binding due to an affinity between bZIP and the DSX^F C-terminus. Repression may occur because the higher self-cooperativity of DSX^M allows it to bind and, through its larger sex-specific C-terminus, sterically exclude bZIP binding.

Putting aside the issue of DSX influence on bZIP transcriptional activation, the fundamental observation of this paper is that although we find little to distinguish between DSX^M and DSX^F binding to the dsxA regulatory site, the sex-specific OD2 domains make crucial dimerization contributions to DNA binding through their physical linkage to the OD1/DBD, the DNA binding domain. Since the OD2 domains appear to be the only other part of full-length protein that make significant contributions to dimerization, we speculate that the dimeric structures of the OD2 domains are necessary for the repression/activation functions of the sex-specific C-termini. If this is the case then the thermodynamic linkage may also work in the other functional direction, namely, from OD1/DBD to the OD2/repression/activation region.

ACKNOWLEDGMENT

We thank Chris Miller and Nobuko Hamaguchi for critical comments on the manuscript and Serge Timasheff for valuable advice.

REFERENCES

1. Tjian, R., and Maniatis, T. (1994) *Cell 77*, 5−8.
2. Triezenberg, S. J. (1995) *Curr. Opin. Genet. Dev. 5*, 190−196.
3. Sauer, F., and Tjian, R. (1997) *Curr. Opin. Genet. Dev. 7*, 176−181.
4. Goodrich, J. A., Cutler, G., and Tjian, R. (1996) *Cell 84*, 825−830.
5. Pugh, B. F. (1996) *Curr. Opin. Cell Biol. 8*, 303−311.
6. Hanna-Rose, W., and Hansen, U. (1996) *Trends Genet. 12*, 229−234.
7. Swillens, S., and Pirsen, I. (1994) *Biochem. J. 301*, 9−12.
8. Jones, N. (1990) *Cell 61*, 9−11.
9. Lamb, P., and McKnight, S. L. (1991) *Trends Biol. Sci. 16*, 417−422.
10. Calkhoven, C., and Geert, A. (1996) *Biochem. J. 317*, 329−342.
11. LeBowitz, J. H., Clerc, R. G., Brenowitz, M., and Sharp, P. A. (1989) *Genes Dev. 3*, 1625−1638.
12. Burtis, K. C., and Wolfner, M. F. (1992) *Semin. Dev. Biol. 3*, 331−340.
13. Taylor, B., Villella, A., Ryner, L., Baker, B., and Hall, J. (1994) *Dev. Genet. 15*, 275−296.
14. Burtis, K. C., and Baker, B. S. (1989) *Cell 56*, 997−1010.
15. An, W., Cho, S., Ishii, H., and Wensink, P. C. (1996) *Mol. Cell. Biol. 16*, 3106−3111.
16. Erdman, S. E., and Burtis, K. C. (1993) *EMBO J. 12*, 527−535.
17. Erdman, S. E., Chen, H. J., and Burtis, K. C. (1996) *Genetics 144*, 1639−1652.
18. An, W., and Wensink, P. C. (1995) *Genes Dev. 9*, 256−266.
19. An, W., and Wensink, P. C. (1995) *EMBO J. 14*, 101−110.
20. Cho, S., and Wensink, P. C. (1996) *Proc. Natl. Acad. Sci. U.S.A. 93*, 2043−2047.
21. Cho, S., and Wensink, P. C. (1997) *J. Biol. Chem. 272*, 3185−3189.
22. Burtis, K. C., Coschigano, K. T., Baker, B. S., and Wensink, P. C. (1991) *EMBO J. 10*, 2577−2582.
23. O'Donnell, K. H., Chen, C.-T., and Wensink, P. C. (1994) *Mol. Cell. Biol. 14*, 6398−6408.
24. Wyman, J., Jr. (1964) *Adv. Protein Chem. 19*, 224−286.
25. Senear, D. F., and Brenowitz, M. (1991) *J. Biol. Chem. 266*, 13661−13671.
26. Cantor, C. R., and Schimmel, P. R. (1980) *Biophysical Chemistry, Vol. 3*, pp 847−876, W. H. Freeman & Co., San Francisco.
27. Coschigano, K. T., and Wensink, P. C. (1993) *Genes Dev. 7*, 42−54.
28. Monini, P., Grossman, S. R., Pepinsky, B., Androphy, E., and Laimins, L. A. (1991) *J. Virol. 65*, 2124−2130.
29. Martinez, E., and Wahli, W. (1989) *EMBO J. 8*, 3781−3791.
30. Brenowitz, M., Jamison, E., Majumdar, A., and Adhya, W. (1990) *Biochemistry 29*, 3374−3383.
31. Brenowitz, M., Mandal, N., Pickar, A., Jamison, E., and Adhya, S. (1991) *J. Biol. Chem. 266*, 1281−1288.
32. Chen, J., and Matthews, K. S. (1994) *Biochemistry 33*, 8728−8735.

BI972916X